Autophagic activation with Nimotuzumab enhanced chemosensitivity and radiosensitivity of esophageal squamous cell carcinoma

Haizhu Song[1], Banzhou Pan[1], Jun Yi[2] and Longbang Chen[1]

[1]Department of Medical Oncology, Jinling Hospital, Medical School of Nanjing University, Nanjing 210002, P.R. China; [2]Department of Cardiothoracic Surgery, Jinling Hospital, Medical School of Nanjing University, Nanjing 210002, P.R. China
Corresponding author: Longbang Chen. Email: Dr.chenlb@163.com

Abstract

Chemotherapy and radiotherapy are two indispensible methods for esophageal squamous cell carcinoma (ESCC), especially for those recurring and metastatic ones, but therapeutic toxicity remains a major problem to overcome. In the present study, the potential therapeutic value of nimotuzumab (an antiepidermal growth factor receptor [EGFR] monoclonal antibody) in combination with chemotherapy and radiotherapy was evaluated on Eca109 and TE-1 ESCC cells, with high and low expression of EGFR, respectively. It was shown that nimotuzumab enhanced the sensitivity of Eca109 cells to other cytotoxic agents (paclitaxel and cisplatinum) and X-ray radiation, and the cytotoxicity was associated with increased autophagy. Conversely, the chemo- and radiosensitivity of TE-1 cells showed no improvement with addition of nimotuzumab, but could be increased by combining with rapamycin, an autophagy inducer. Therefore, it was concluded that autophagic activation mediated by nimotuzumab could promote autophagic cell death and produce additive antitumor effects.

Keywords: Autophagy, chemotherapy, radiotherapy, epidermal growth factor receptor, esophageal squamous cell carcinoma

***Experimental Biology and Medicine* 2014; 239: 529–541. DOI: 10.1177/1535370214525315**

Introduction

Esophageal cancer is an aggressive cancer, being rated the sixth most common cause of cancer-related mortality among malignancies worldwide.[1] It is mainly classified into squamous cell carcinoma and adenocarcinoma, and the former is more prevalent in East Asia while the latter is more common in western countries. Although progressive studies have been conducted on the treatment of esophageal squamous cell carcinoma (ESCC), the prognosis for patients with advanced esophageal carcinoma remains extremely poor, with only a 5–6 months median overall survival time.[2,3] Surgery is the main option for locally advanced esophageal carcinoma, but results in a 5-year survival rate of only 20–25%.[4] The benefits of chemotherapy and radiotherapy as adjuvant treatments are still controversial, as the therapeutic toxicity continues to be a major problem. Therefore, new effective therapeutic approaches with minimal toxicity are imminently needed.

Substantial evidence has confirmed the pivotal role of epidermal growth factor receptor (EGFR) in various cancer models, including ESCC. Overexpression of EGFR has been shown to be correlated with cell proliferation, survival, invasion, and migration[5,6] and has an inverse relationship to anticancer therapeutics.[7] Recently, a combination of EGFR inhibitors and chemotherapy or radiotherapy has been reported to improve local tumor control effectively, compared to cytotoxic agents or irradiation alone.[8,9] These findings may provide a reasonable therapeutic approach based on EGFR-targeting therapy in combination with adjuvant chemotherapy or radiotherapy.

Autophagy, also called macroautophagy, is a highly conserved intracellular self-digestion process that entails the degradation of proteins and organelles to maintain cellular homeostasis.[10] Of note, the specific role of autophagy in cancer is double-sided and context-dependent. Autophagy has been implicated as not only a cytoprotective mechanism in response to cancer therapy, but also a direct cell death mechanism for contribution to increase the chemosensitivity and radiosensitivity.[11] On account of the seemingly conflicting double roles, autophagy has emerged as a focus of intense research efforts, suggesting a potential therapeutic target to improve the existing therapies.

Nimotuzumab is a humanized anti-EGFR monoclonal antibody that competes for EGF binding to the extracellular domain of EGFR, thus inhibiting EGF-stimulated receptor autophosphorylation and downstream signaling pathways.[12] The antiproliferative activity of nimotuzumab has been approved in clinical trials for various tumor types.[13,14]

The majority of investigations have focused on the therapeutic effects of nimotuzumab on cancer cells including cell cycle arrest and the induction of apoptotic cell death.[15,16] However, few previous studies have investigated autophagy induced by nimotuzumab. In the current study, we report that nimotuzumab could enhance the response of ESCC cells with high EGFR expression to paclitaxel (PTX), cis-platinum (DDP), and external beam radiation through activating autophagy. Notably, in cells insensitive to nimotuzumab, autophagy was not activated, and addition of nimotuzumab had little effect on chemosensitivity and radiosensitivity. Nevertheless, induction of autophagy by mammalian target of rapamycin (mTOR) inhibitor rapamycin could increase the sensitivity of these insensitive cells to both chemo- and radiotherapy. These findings suggested that activation of autophagy may be an effective strategy in increasing chemosensitivity and radiosensitivity of ESCC.

Materials and methods

Cell line and reagents

Two esophageal squamous cell lines (Eca109 and TE-1) were purchased from the Tumor Cell Bank of the Chinese Academy of Medical Science (Shanghai, China) and maintained in RPMI 1640 medium containing 10% calf serum and ampicillin and streptomycin at 37°C in a humidified atmosphere of 95% air and 5% CO_2. The following antibodies used for Western blot analysis were purchased from Cell signaling: EGFR, LC-3, poly(ADP-ribose) polymerase (PARP), cleaved-PARP (c-PARP), caspase3, activated-caspase3 (c-caspase3), Atg5. All the other chemical reagents and solvent were purchased from Sigma-Aldrich (St. Louis, MO).

Immunocytochemical staining

The procedure of EGFR examination on ESCC cells included immunocytochemical staining and Western blot analysis, as follows. Briefly, for the immunocytochemical staining, firstly, cells grown on a sterile glass cover slide were fixed with a 10% neutral-buffered formalin solution for 10 min. Next after fixation, endogenous peroxidase activity was blocked with 0.3% hydrogen peroxide for 15 min. Non-specific binding was blocked with 10% normal rabbit serum for 20 min. The slides were then incubated first with a rabbit antibody against the EGFR for 60 min and then with a biotinylated rabbit anti-mouse immunoglobulin at a concentration of 1:100 for 30 min at 37°C. The slides were then reacted with a streptavidin–peroxidase conjugate for 30 min at 37°C and with 3′-3′-diaminobenzidine as a chromogen substrate. Finally, the nucleus was counterstained using Meyer's hematoxylin. Cells were observed under a microscope.

cDNA constructs, siRNA, and transfection

The green fluorescent protein-tagged (GFP-tagged) LC3 cDNA expression construct was a gift from Dr Noboru Mizushima (Tokyo Medical and Dental University, Tokyo, Japan). A 21-mer siRNA oligonucleotide duplexes targeting Atg5 (siRNA/Atg5): sense sequence, 5′-GCUAUAUCAGGAUGAGAUATT-3′; antisense sequence, 5′-UAUCUCAUCCUGAUAUAGCGT-3′ and the negative control siRNA(siRNA/NC): sense sequence, 5′-UUCUCCGAACGUGUCACGUTT-3′; antisense sequence, 5′-ACGUGACACGUUCGGAGAATT-3′ were chemically synthesized by GenePharma (Shanghai, China). The cDNA construct and the siRNA oligonucleotide were transfected into the targeted cells with Lipofectamine 2000 (Invitrogen) according to the manufacturer's instructions. We determined the efficiency of siRNA-mediated protein knockdown by Western blot analysis.

Western blot analysis

The whole cell lysates were separated on sodium dodecyl sulfate polyacrylamide gel electrophoresis (SDS-PAGE) and electrophoretically transferred to polyvinylidene difluoride (PVDF) membranes. Blots were blocked for about 2 h in tris buffered saline with tween20 (TBST) containing 5% skim milk or bovine serum albumin (BSA), followed by at least 2 h incubation at room temperature or overnight or 4°C with the desired primary antibodies. Then blots were washed three times with TBST and incubated for 2 h at room temperature with the secondary antibodies (horseradish peroxidase (HRP)-conjugated goat anti-rabbit or anti-mouse IgG, Jackson Research Labs). Immunoreactive bands were visualized by an enhanced chemiluminescence detection kit.

Methylthiazolyldiphenyl-tetrazolium bromide (MTT) survival assay

Cells were seeded at 5×10^3/well in 96-well plates in a final volume of 100 μL and treated with the desired drug or drug combination for 48–72 h. Then 20 μL of MTT (5 mg/mL) was added to each well and incubated for 4 h at 37°C, after MTT was removed, 100 μL of dimethyl sulfoxide (DMSO) was added per well to solubilize the formazan product. The relative number of surviving cells in each group was determined by measuring the optical density of the cell lysates at 560 nm.

Apoptosis assay

We measured apoptosis by using an annexin-V–fluorescein isothiocyanate apoptosis detection kit (Oncogene Research Products, Boston, MA) via flow cytometric analysis that quantitatively measures the percentage of early apoptotic cells and by Western blot analysis with antibodies that recognize c-PARP and c-caspase3 after various treatments.

Radiosensitivity assay

A colony formation assay was used to detect radiosensitivity. Cells were plated in triplicate (800/well) in six-well plates for about 24 h under standard conditions. After specific treatments, the cells were then irradiated with different doses of X-ray radiation (0–2–4–6–8 Gy). Twenty-four hours after irradiation, the medium was replaced with fresh one. After 14 days of incubation, the colonies were fixed with methanol, stained with 0.5% crystal violet in absolute ethanol and colonies with $\geq$50 cells were counted under dissection microscope. In each irradiation dose group, the surviving fraction of cells was calculated as plating efficiency of the irradiated cells divided by the plating efficiency of the irradiated cells by that of mock control.

Immunofluorescence microscopy

Cells transfected with the GFP-LC3 cDNA constructs were grown in 12-well plates and then treated with the desired drugs or drug combination. For immunofluorescence processing, cells were washed twice with phosphate buffer solution (PBS) and fixed for 15 min at room temperature in 4% paraformaldehyde. The cells were finally observed by using a fluorescence microscope.

Transmission electron microscopy

After treatment with a solution containing 3% glutaraldehyde plus 2% paraformaldehyde in 0.1 mol/L PBS (pH 7.3) for 1 h, cell suspension samples were washed and fixed with 0.1% buffered osmium tetroxide for 30 min, stained with 1% Millipore-filter uranyl acetate, dehydrated in increasing concentrations of ethanol, infiltrated, and embedded in LX-112 medium. Then, the samples were polymerized in a 70°C oven for 2 days. Ultrathin sections were cut with a Leica Ultra cut microtome, stained with uranyl acetate and lead citrate in a Leica EM stainer, and examined with a JEM 1010 transmission electron microscope at an accelerating voltage of 80 kV. Digital images were obtained using an advanced microscopy techniques imaging system.

Statistical analysis

Data were presented as mean ± SD from at least three separate experiments. Unpaired Student's *t*-test was used to evaluate differences between the control group and each treatment group, with the resultant *P* representing a two-sided test of statistical significance. SPSS 17.0 (SPSS, Inc., Chicago, IL) was used for statistical analyses with a *P* value of <0.05 considered statistically significant.

Results

Synergistic effect of nimotuzumab-containing chemotherapy on ESCC cells

In our initial study, the EGFR expression of TE-1 and Eca109 esophageal cancer cells was examined under basal conditions. As shown in Figure 1(a) and (b), we found that Eca109 cells expressed a significantly higher level of EGFR than TE-1 cells.

Firstly, we examined the chemotherapeutic-induced cytotoxic effects of nimotuzumab (h-R3) in ESCC cells.

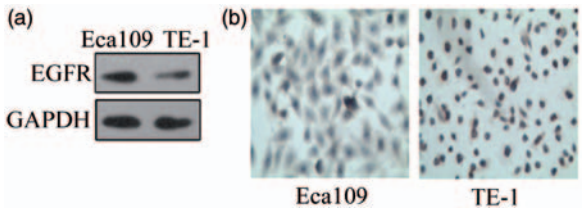

Figure 1 Comparison of EGFR expression levels in ESCC Eca109 and TE-1 cells. (a) EGFR expression was analyzed by Western blot analysis. (b) Immunocytochemical staining of expression of EGFR in both cells. Eca109 cells (left) and TE-1 cells (right). Representative areas were photographed and shown (×100 magnification). (A color version of this figure is available in the online journal.)

Nimotuzumab showed no toxicity to either Eca109 or TE-1 cells, even when they were treated with 400 μg/mL nimotuzumab for 48 h ($P>0.05$), as determined by the MTT assay (Figure 2(a)). Next, these two ESCC cell lines were employed for testing the efficacy of nimotuzumab combined with PTX or DDP. The amount of metabolically active cells treated in the absence and presence of nimotuzumab, respectively, was determined as shown in Figure 2(b) to (e). The IC50 of PTX or DDP was displayed under various conditions (Table 1). Pretreatment of 200 μg/mL nimotuzumab for 48 h effectively decreased the IC50 of both PTX and DDP in Eca109 cells. However, this effect could not be highly improved by increasing the dose of nimotuzumab to 400 μg/mL. Conversely, no enhanced antitumor effect was observed at any of the different dosages for TE-1 cells.

Nimotuzumab-enhanced chemosensitivity is not mediated through apoptosis

To explore the potential mechanism whereby nimotuzumab enhanced the sensitivity to other cytotoxic agents, single drug and their combinations were tested for their ability to promote apoptosis in both cells. We used suboptimal doses of both cytotoxic agents (0.19 μg/mL PTX and 1.5 μg/mL DDP), which only induced a modest level of apoptosis, allowing us to detect the increased degree of apoptotic activity after nimotuzumab combination. Flow cytometric analysis of externalized phosphatidylserine suggested that the early apoptotic rate of Eca109 cells was mildly increased after addition of nimotuzumab at doses of 400 μg/mL, as well as the expression of activated caspase3 (c-caspase3) and c-PARP, two main markers of apoptosis, compared with PTX or DDP monotherapy (Figure 3(a) and (c)). No significant improvement of the apoptosis rate on the addition of nimotuzumab was observed in TE-1 cells (Figure 3(b) and (d)). It was found that 200 μg/mL nimotuzumab significantly enhanced the sensitivity to PTX and DDP, as presented in Table 1, so that the slight increase of type I apoptosis is most likely not the main reason for the chemosensitized effect displayed by Eca109 cells, and the cytotoxicity elicited by nimotuzumab-containing chemotherapy is likely to involve a distinct mechanism of cell death.

Nimotuzumab potentiates autophagic cell death when combined with chemotherapy

Having excluded the programmed cell death type I from modulating the cytotoxicity of drug combination, we next evaluated the effect of nimotuzumab alone or combination treatment on the induction of autophagy.

The first assay for autophagy relied on the detection of the conversion from microtubule-associated protein 1 light chain3-I (LC3-I) to the phosphatidylethanolamine-conjugated form (LC3-II), an indicator of increased autophagic activity. Treatment of Eca109 cells with nimotuzumab induced LC3-II conversion in a dose-dependent manner. However, no significant LC3-II induction patterns have been observed in TE-1 cells with EGFR low expression (Figure 4(a)). Similar results were found after transfection

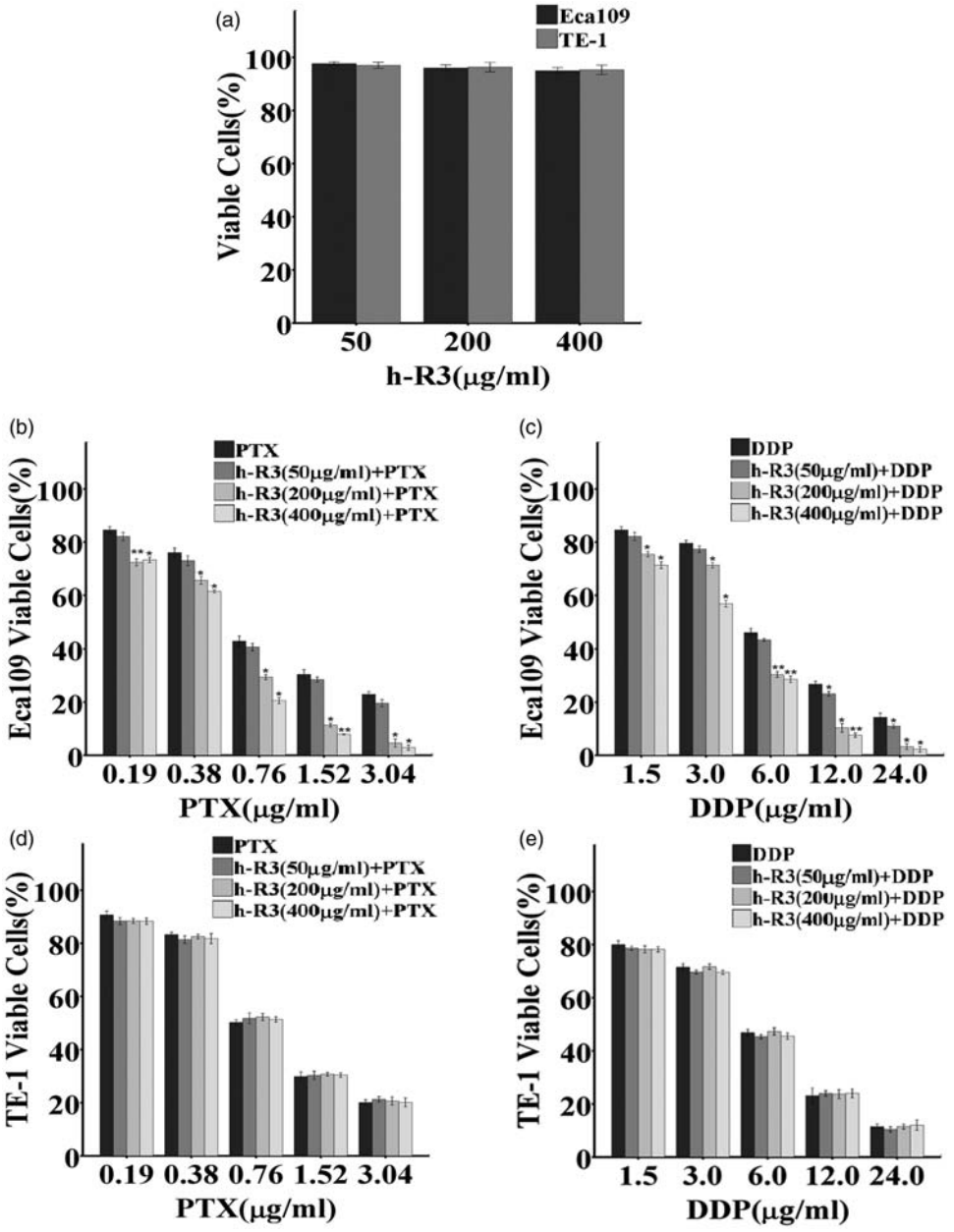

Figure 2 Synergistic effect of nimotuzumab combined with PTX or DDP on ESCC cells. (a) The percentage of viable cells of Eca109 or TE-1 cells cultured with nimotuzumab (h-R3) at the indicated concentrations for 48 h were examined by MTT assay. (b to e) Eca109 and TE-1 cells were incubated with or without nimotuzumab (50, 200, or 400 μg/mL) for 48 h and exposed to the indicated dose of paclitaxel (PTX) or cis-platinum (DDP) for 72 h, and then the cell viability was analyzed by MTT assay. The experiments were performed in triplicate. $N = 3$, means ± SD, $^{*}P < 0.05$, $^{**}P < 0.01$, compared with the groups of PTX or DDP alone

of these cells with a cDNA construct containing GFP-LC3, which could convert from a diffuse cytoplasmic fluorescence to a punctate or 'dot-like' pattern once autophagy is induced. In Eca109 cells transfected with GFP-LC3 constructs, more punctate fluorescent dots were noticed after nimotuzumab treatment when compared with untreated cells, which suggests that LC3-II conversion is actively occurring. Moreover, the number of cells with punctate fluorescence was quantified to estimate the level of autophagosome formation (Figure 4(b)). The induction of autophagy by nimotuzumab in Eca109 cells was also confirmed by transmission electron microscopy, which showed an abundance of characteristic autophagosomes (Figure 4(c)). Since LC3-II can be degraded by the lysosome along with autophagosomal cargo, we treated Eca109 cells with an autophagy-lysosomal inhibitor, bafilomycin A1, for 2 h prior to harvesting of lysates, so as to better assess the dynamic process of autophagic flux induced by nimotuzumab. We observed that LC3-II accumulation, in the presence of bafilomycin A1, was higher in Eca109 cells treated with nimotuzumab than in carrier controls (Figure 4(d)).

We subsequently found that co-treatment of nimotuzumab in conjunction with PTX or DDP continued to induce a higher accumulation of LC3-II (Figure 5(a)). Again, the

Table 1 IC50 of nimotuzumab combined with PTX or DDP on inhibition of ESCC cells growth

	IC50 (μg/mL)	
Compound treatment	**Eca109**	**TE-1**
PTX	0.69 ± 1.02	0.77 ± 1.28
PTX + h-R3 (50 μg/mL)	0.61 ± 0.97	0.81 ± 0.68
PTX + h-R3 (200 μg/mL)	0.45 ± 0.74**	0.86 ± 0.74
PTX + h-R3 (400 μg/mL)	0.41 ± 0.86**	0.84 ± 1.24
DDP	5.83 ± 0.66	5.71 ± 0.83
DDP + h-R3 (50 μg/mL)	5.27 ± 0.59	5.20 ± 0.95
DDP + h-R3 (200 μg/mL)	3.23 ± 0.52*	5.82 ± 0.67
DDP + h-R3 (400 μg/mL)	3.08 ± 0.43**	5.43 ± 1.02

Eca109 and TE-1 cells were exposed to nimotuzumab (50, 200, or 400 μg/mL), and PTX or DDP was added after nimotuzumab for 48 h as indicated, and the cell viability was detected by MTT assay. Values were reported as mean ± SD of three independent experiments, *$P<0.05$, **$P<0.01$, significant difference of the treatment with two drugs versus single drug calculated by Student's *t*-test.

administration of both agents to these cells was more efficient in inducing punctate GFP fluorescent dots than that of either alone (Figure 5(b)). Figure 5(c) further shows the changes in the survival rate of Eca109 cells measured with a MTT assay. Nimotuzumab sensitized Eca109 cells to PTX or DDP, respectively, as the combination of nimotuzumab led to more cell death than either treatment alone. However, the effect of nimotuzumab on chemosensitivity was abrogated by knockdown of Atg5, a critical autophagy protein, suggesting that the effects of nimotuzumab on chemosensitivity are modulated through autophagy. To further demonstrate that the enhanced cell death induced by the combination treatment was caused by an increase in autophagic activity, we co-treated Eca109 cells with 20 μM Z-VAD-fmk (benzyloxycarbonyl Val-Ala-Asp(O-methyl)-fluoro-methylketone), a pan-caspase inhibitor.[17] As shown in Figure 5(d), addition of Z-VAD-fmk did not inhibit the cell death induced by nimotuzumab and chemotherapeutic co-treatment. This result strongly suggests that autophagy induced after nimotuzumab-containing chemotherapy may function as a direct cell death execution mechanism.

Meanwhile, we analyzed the induction of autophagy by co-treatment of nimotuzumab and the two cytotoxic agents in TE-1 cells. As we expected, compared with the response of TE-1 cells to PTX or DDP monotherapy, addition of nimotuzumab at all doses failed to further increase the LC3-II level (Figure 6(a)). To confirm the effect of nimotuzumab-induced autophagy on chemosensitivity, we pretreated TE-1 cells with rapamycin, a well-known inducer of autophagy through inhibition of mTOR,[18] to mimic the role of nimotuzumab in the induction of autophagy. A higher level of LC3-II accumulation can be observed in TE-1 cells treated with both agents than either alone. Besides, we found that the combination treatment had no appreciable effect on the PTX or DDP-induced PARP cleavage and caspase3 activation (Figure 6(b)). Similar to the results from the Eca109 cells, co-treatment of TE-1 cells with rapamycin and either of the two cytotoxic drugs substantially reduced the relative number of surviving cells in comparison to one drug monotherapy. Then, knockdown of Atg5 greatly deprived the effect of rapamycin on chemosensitivity, which strongly suggests that the increased cell death induced by co-treatment stems mainly from autophagic cell death (Figure 6(c)).

Together, these data suggest that, if autophagy could be activated and the activity be kept at an elevated baseline level, an increased amount of cell death would be achieved after conventional chemotherapy for autophagic cell death.

Nimotuzumab improves radiosensitivity via activation of autophagy

Combination of radiotherapy and EGFR inhibitors was reported to improve local tumor control compared to irradiation alone, but the underlying mechanism is less well understood. To determine whether or not nimotuzumab improved ESCC cell radiosensitivity, we treated both Eca109 and TE-1 cells with increasing doses of nimotuzumab and then exposed them to radiation doses ranging from 0 to 8 Gy (Figure 7(a) and (b)). From the results confirmed of the colony formation assay, combination treatment of Eca109 cells revealed a mild reduction of survival rate at 2 Gy dose of X-ray, and addition of 400 μg/ml nimotuzumab maximized the gap of cell viability under the 4 Gy dose of irradiation. Similarly, nimotuzumab had no effect on the radiosensitivity of TE-1 cells.

Next, we further examined both the levels of apoptosis and autophagy in these two cells treated with or without nimotuzumab before radiotherapy. In Eca109 cells, we observed that only a 4 Gy dose of irradiation combined with 400 μg/mL nimotuzumab can result in a modest increase of annexin-V/PI positive cells by 3.98% (SD ± 0.13) as compared to the X-ray alone group (Figure 7(c)). Western blot analysis of c-caspase3 and c-PARP further confirmed the result (Figure 8(a)). For the detection of the autophagy level, we assessed the appearance of LC3-II by using a fluorescent microscope and by Western blot analysis as shown in Figure 8(a) and (c). Nimotuzumab excited additive effects on the accumulation of LC3-II for Eca109 cells, in combination with radiotherapy even at 2 and 4 Gy doses. However, TE-1 cells displayed no increase in either levels of apoptosis or autophagy in all the groups of combination treatment (Figures 7(d) and 8(b)).

To further confirm that the radiosensitizing effect of nimotuzumab is also caused by the activation of autophagy, we firstly inhibited autophagy by silencing Atg5 in Eca109 cells (Figure 8(d)). This effect was reversed as we expected. Then we also treated TE-1 cells with rapamycin before radiotherapy. Similar to our results in Figure 6(c), rapamycin-induced autophagy further decreased the survival rate by 14.22% (SD ± 0.80), 32.30% (SD ± 0.94), 18.65% (SD ± 0.47), in comparison with 2, 4, 6 Gy doses of X-ray alone, respectively. After knockdown of Atg5, additive cell death induced by rapamycin was inhibited (Figure 8(e)).

Discussion

Clinically, chemotherapy and radiotherapy are two indispensible methods for ESCC, especially for those recurring and metastatic ones. However, there is need to address the challenge of developing new strategies that could enhance

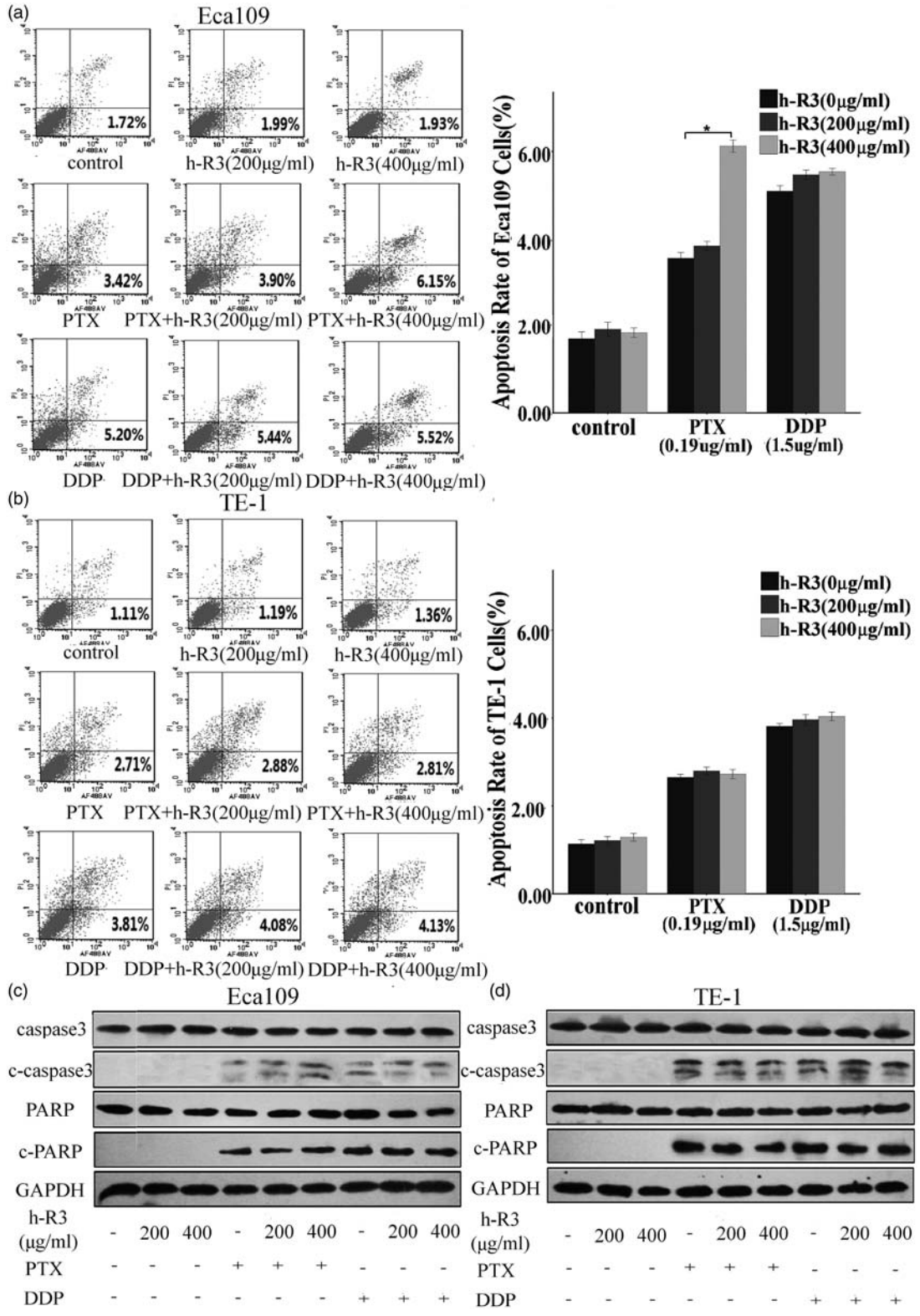

Figure 3 Analysis of apoptosis in Eca109 and TE-1 cells received nimotuzumab-containing treatments. (a, b) Eca109 and TE-1 cells were treated for 48 h in the presence of nimotuzumab (200 and 400 μg/mL), PTX (0.19 μg/mL) or DDP (1.5 μg/mL), or combination and then processed for fluorescence activated cell sorter (FACS) by using annexin-V/PI staining. (c, d) Cell lysates were prepared for the Western blot analysis of total caspase3, activated caspase3 (c-caspase3), total PARP, and cleaved-PARP (c-PARP). GAPDH was used as an internal control. For all the experiments, image shown is representative of three replicates

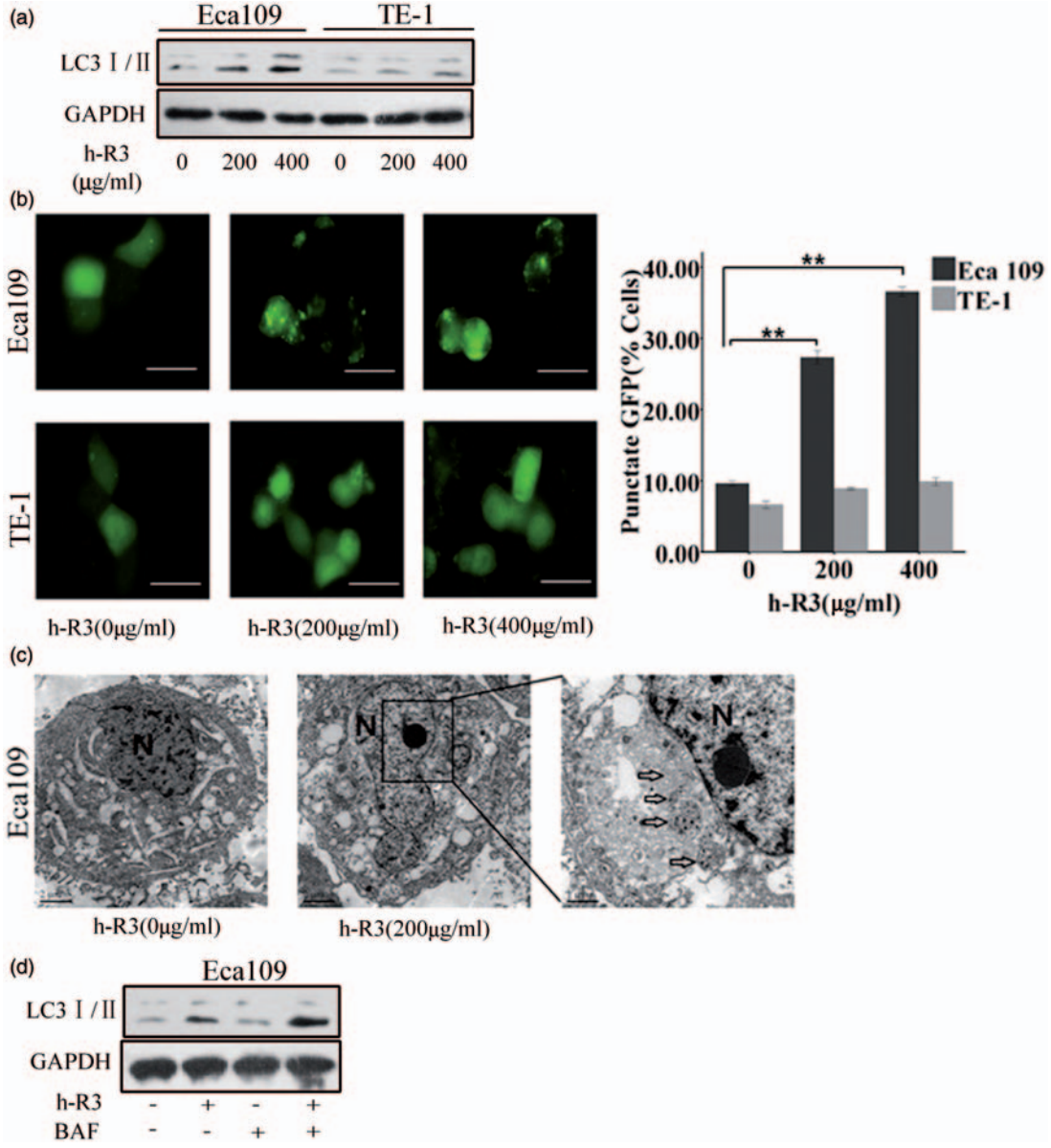

Figure 4 Nimotuzumab induced autophagosome formation and increased autophagic flux in EGFR high-expressed Eca109 cells. (a) Eca109 and TE-1 cells were treated with nimotuzumab (200 and 400 μg/mL) or carrier control for 48 h. Total cell lysates were subjected to Western blot test for LC3 and GAPDH. (b) Nimotuzumab induced appearance of the membrane-associated LC3 (punctate fluorescence) in Eca109 cells. Both ESCC cells were transiently transfected with GFP-LC3 constructs for 24 h and then treated with or without nimotuzumab (200 and 400 μg/mL) as indicated for 24 h. The number of cells with punctate fluorescence was counted in 10 different fields under a fluorescent microscope and is shown as a percentage of the total number of cells counted. Bar = 50 μm. (c) Nimotuzumab induced the formation of autophagosomes in Eca109 cells. Eca109 cells were either untreated or treated with 200 μg/mL nimotuzumab Eca109 cells for 24 h. Cell samples were prepared for transmission electron microscopy as described in 'Materials and methods' section. A magnified view of the electron photomicrograph showed the characteristic autophagosomes. N = nucleus. (d) Inhibition of the autophagic flux led to accumulation of nimotuzumab-induced LC3-II in Eca109 cells. Eca109 cells were either untreated or treated with 200 μg/mL nimotuzumab for 48 h in the absence or presence of bafilomycin A1 (BAF, 40 nM). Whole cell lysates were analyzed by Western blot. GAPDH was used as a protein loading control. The results were obtained from three independent experiments. Values shown in B are means ± SD, ** $P<0.01$. (A color version of this figure is available in the online journal.)

chemosensitivity and radiosensitivity without adding further therapeutic toxicity on normal tissues. Combination therapies, in particular signaling-directed combination treatments such as targeting the EGFR signaling pathway, have received much attention in recent years.[19] Several studies have demonstrated that EGFR inhibitors could further improve the efficacies of other cytotoxic treatments, providing a category of additional agents in anticancer therapies.[20,21]

Nimotuzumab is a humanized IgG1 isotype monoclonal antibody targeting EGFR, and previous studies have confirmed its antitumor effect in brain[22] and non-small cell lung cancer cells[23] with high or moderate levels of EGFR expression. Recent studies focused on assessing the antitumor efficacy of nimotuzumab and cetuximab (another humanized anti-EGFR mAb) in human breast adenocarcinoma and lung adenocarcinoma cells, and it was summarized that the antitumor effect of nimotuzumab decreased

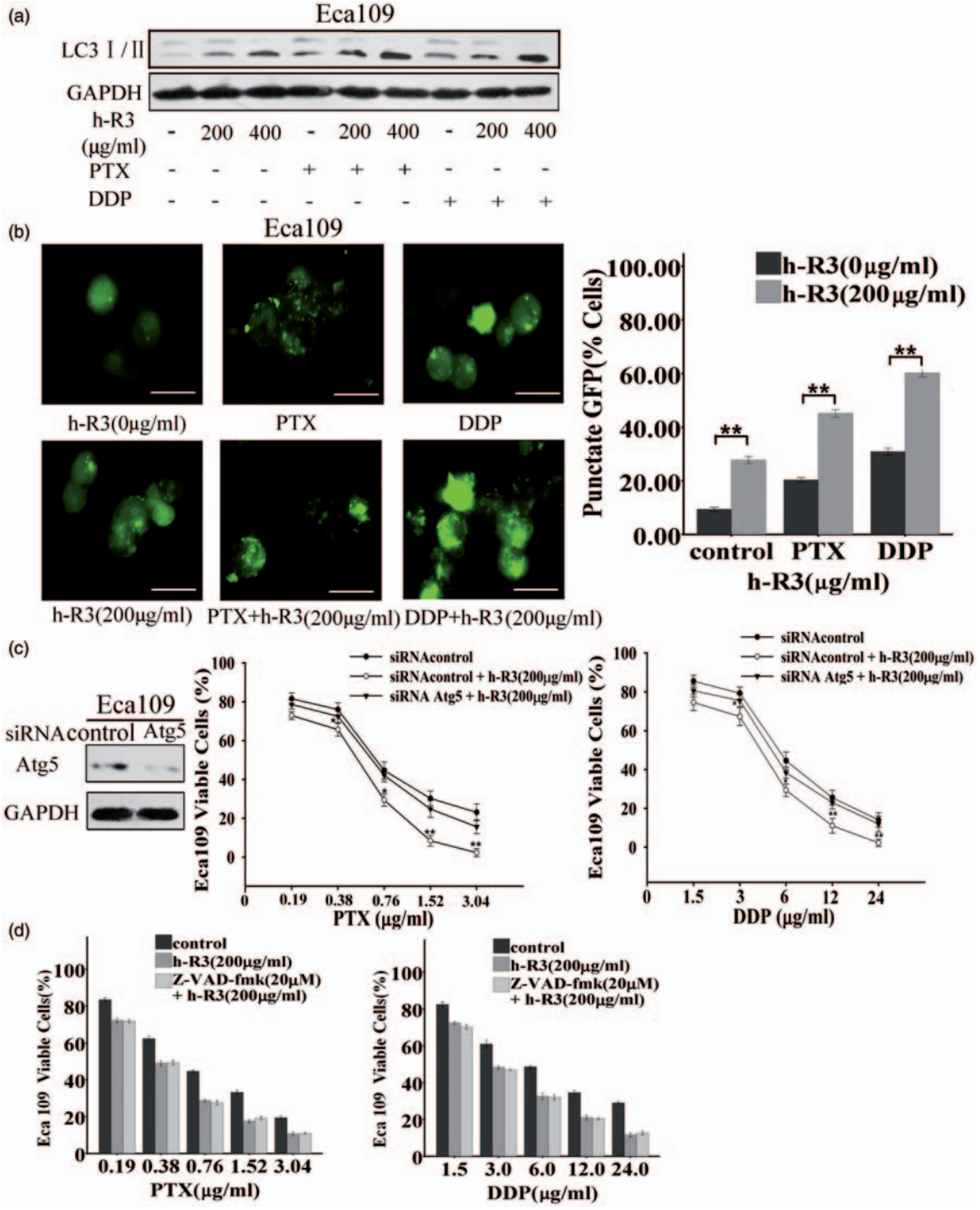

Figure 5 Nimotuzumab increased autophagic cell death when combined with PTX or DDP in Eca109 cells. (a) Eca109 cells were treated with PTX (0.19 μg/mL) or DDP (1.5 μg/mL), in the presence or absence of nimotuzumab (200 and 400 μg/mL) for 48 h. Cell lysates were subjected to Western blot for LC3-II accumulation. (b) Eca109 cells that transiently transfected with GFP-LC3 constructs were treated with nimotuzumab (200 μg/mL), PTX (0.19 μg/mL) or DDP (1.5 μg/mL), or both agents treatments for 24 h. The number of cells with punctate fluorescence was counted as in Figure 4(b). Bar = 50 μm. (c) Eca109 cells were transiently transfected with siRNA against Atg5 or control siRNA for 48 h. After transfection, cells with and without Atg5 knockdown were exposed to 200 μg/mL nimotuzumab and either of PTX or DDP for 72 h as indicated. Viable cells were determined with an MTT assay. (d) Cell viability was determined by annexin-V/PI through flow cytometry after treatment with control (1:1000 DMSO), 200 μg/mL h-R3, 20 μM Z-VAD-fmk with 200 μg/mL h-R3, in combination with PTX or DDP as indicated. (A color version of this figure is available in the online journal.)

together with the EGFR expression level while cetuximab did not.[24] In contrast, in our studies, nimotuzumab alone seemed not to have any cytotoxic effect, neither on the EGFR high-expression cells (Eca109) nor on the EGFR low-expression cells (TE-1). However, non-cytotoxic doses of nimotuzumab (both 200 and 400 μg/mL) dramatically enhanced cytotoxic treatments of PTX and DDP responses of Eca109 cells. Then we attempted to investigate the

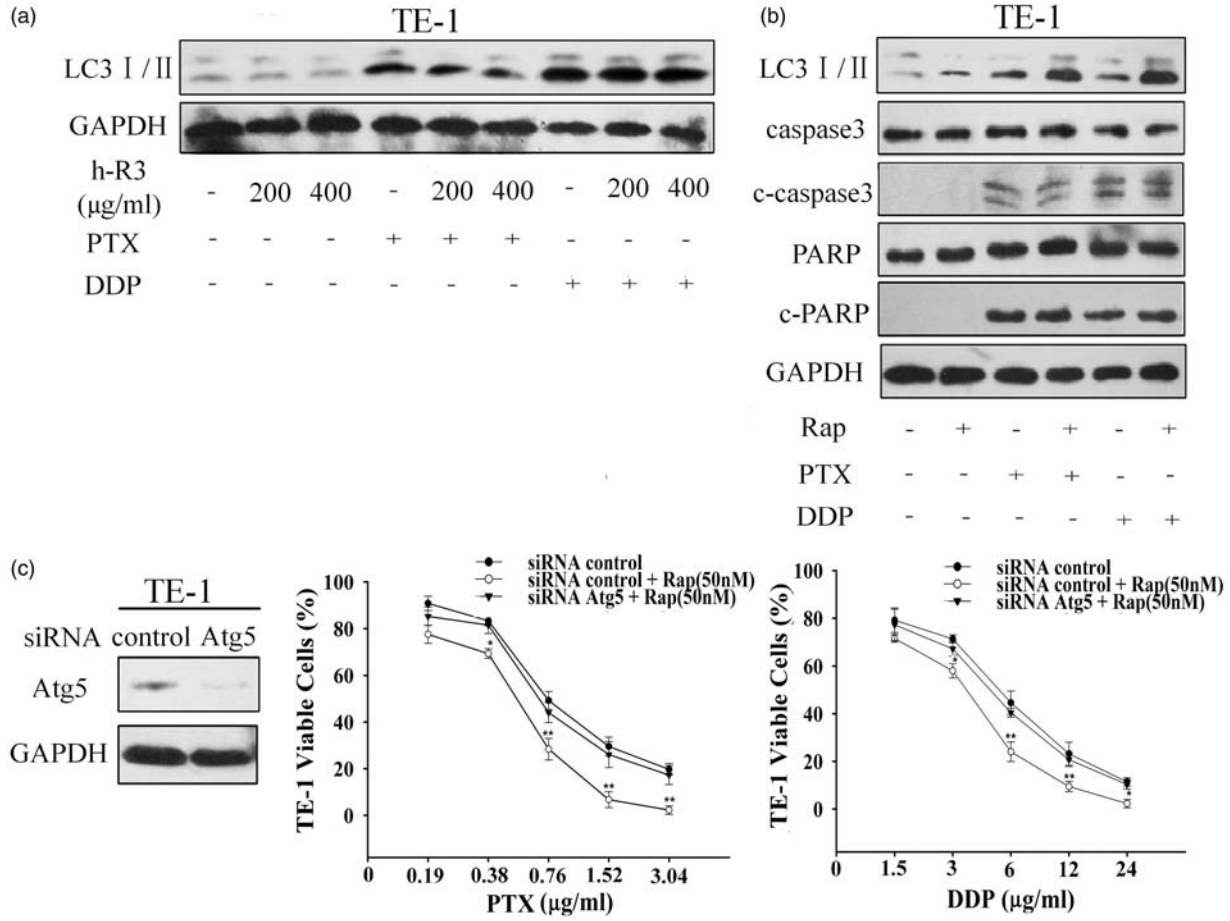

Figure 6 Rapamycin enhanced TE-1 cells autophagic cell death in combination with PTX or DDP treatment. (a) TE-1 cells were treated with nimotuzumab (200 and 400 μg/mL), PTX (0.19 μg/mL) or DDP (1.5 μg/mL), or combination therapy as in Figure 5(a). (b) TE-1 cells were treated with carried control (1:1000 DMSO), 50 nM rapamycin, 0.19 μg/mL PTX or 1.5 μg/mL DDP, or both agents for 48 h as indicated. Cell lysates were subjected to Western blot for LC3-II accumulation, total caspase3, activated caspase3 (c-caspase3), total PARP, and c-PARP. (c) Forty-eight hours after TE-1 cells were transfected with siRNA Atg5 or siRNA control, both cells with or without Atg5 knockdown were treated with 50 nM rapamycin (Rap) plus PTX or DDP for 72 h

antitumor mechanism of nimotuzumab-containing chemotherapy and radiotherapy. Treatment of Eca109 cells with 400 μg/mL nimotuzumab for 48 h revealed only a slight improvement of apoptosis rate and caspase activation, in the presence of other cytotoxic agents (PTX or DDP) or X-ray, but nimotuzumab at a dose of 200 μg/mL for 48 h showed significantly increased chemosensitivity and radiosensitivity. These results suggested that another non-apoptotic cell death pathway might exist.

In the later study, our data showed a significant increase in autophagy after a combinational therapy for nimotuzumab. This finding is consistent with the recent report that gefitinib (an EGFR tyrosine kinase inhibitor) could efficiently increase docetaxel cytotoxicity in oral squamous cell carcinoma cell lines via mediating autophagic cell death.[25] Nimotuzumab alone caused a dose-dependent formation of LC3-II in Eca109 cells, which was also confirmed by transmission electron microscopy and immunofluorescence microscopy analysis. Also, pretreatment of 200 μg/ml nimotuzumab for 48 h prior to other cytotoxic therapeutics promoted extensive perinuclear accumulation of LC3-II and the appearance of dense autophagosomes. The question of whether the induction of autophagy should be considered as a direct cell death pathway or a cytoprotective mechanism for long time survival remains a controversial topic. In our model, autophagic activation by nimotuzumab facilitated the antitumor effects of cytotoxic agents and irradiation, as shown by two points: first, both the concentration of agents and the dose of irradiation, which significantly inhibited cell survival, could be reduced by at least 1.5-fold; second, maximal cytotoxicity increased. Meanwhile, a blockade of autophagic activity via Atg5 knockdown reduced the cytotoxic effect of adding nimotuzumab to either agent or irradiation. Moreover, a broad-spectrum caspase inhibitor was taken to rule out cytotoxic agent-induced apoptosis that contributed to cell death. Surprisingly, in TE-1 cells, which only exhibited poor induction of autophagy in response to nimotuzumab, combination treatment with rapamycin and adjuvant chemotherapy or radiotherapy can bring about an apparent increase of autophagic activation while also producing more profound cell death than any single agent alone. Similarly, this increase in numbers of dead cells was also suppressed by silencing Atg5. Therefore, nimotuzumab-induced autophagic activation impels cells to enter autophagic cell death pathway.

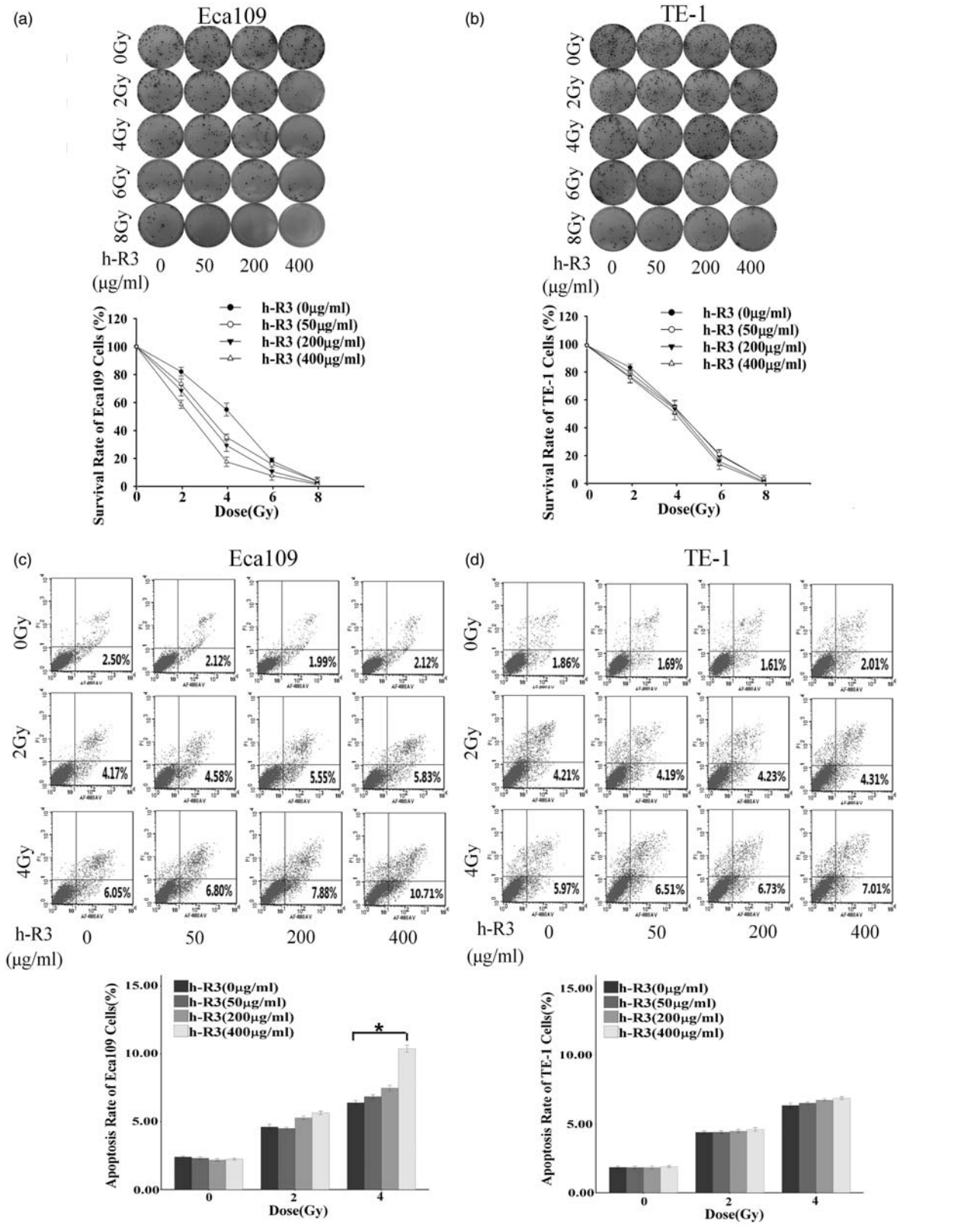

Figure 7 Nimotuzumab increased radiosensitivity in Eca109 cells. (a, b) Eca109 and TE-1 cells were incubated with or without nimotuzumab (50, 200, or 400 μg/mL) for 48 h and exposed to the indicated doses of radiotherapy (RT). The colonies were stained and counted, and survival curves were constructed from three independent experiments. (c, d) Both cells were treated with RT (2 and 4 Gy) in presence or absence of nimotuzumab (50, 200, or 400 μg/mL) for 48 h. Cell lysates were analyzed by an apoptosis assay as in Figure 3(a)

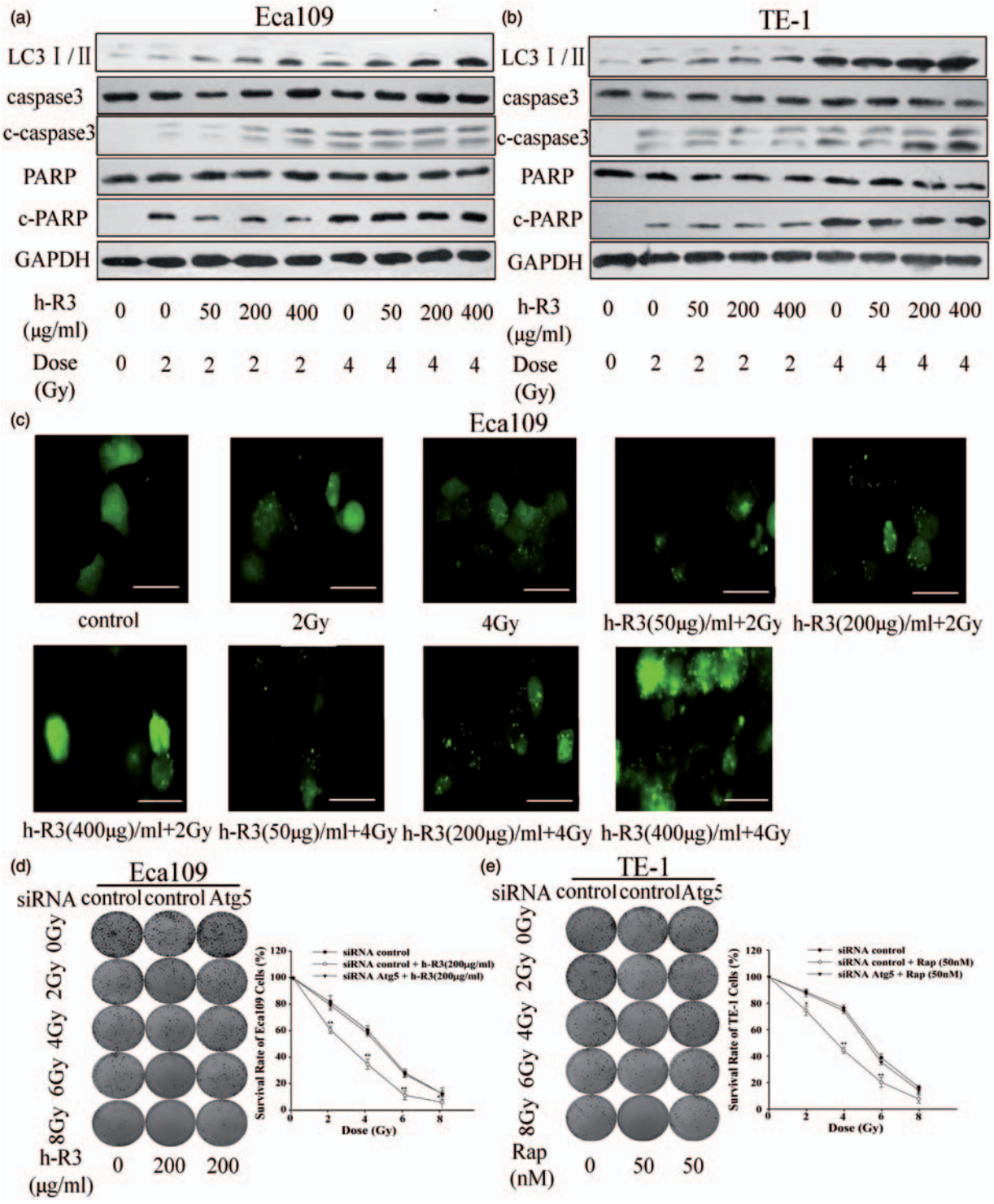

Figure 8 Autophagic activation mediated by nimotuzumab promoted autophagic cell death. (a, b) Both cells were treated as in Figure 7(c) and (d), then total cell lysate was tested by Western blot analysis for LC3-II accumulation, total caspase3, activated caspase3(c-caspase3), total PARP, and c-PARP. (c) After transfected with GFP-LC3 constructs for 24 h, Eca109 cells were exposed to 2 or 4 Gy doses of RT in the presence of nimotuzumab (50, 200, or 400 μg/mL) for 24 h. Bar = 50 μm. Eca109 and TE-1 cells that were transfected with siRNA Atg5 or siRNA control construct were treated with RT with 200 μg/mL nimotuzumab (d) or RT with 50 nM rapamycin (e), respectively. Colonies were stained and counted. (A color version of this figure is available in the online journal.)

For further research, it is worth probing into the mechanism whereby nimotuzumab activates autophagy. Previous studies have shown that nimotuzumab could only selectively bind to tumor cells that expressed moderate to high levels of EGFR and then specifically inhibit EGFR activation.[24] In our studies, it seemed that whether nimotuzumab could induce autophagy or not also depends on the level of EGFR expression. As shown in Figure 4(a) and (b), high-expressed Eca109 cells provoked an abundant formation of autophagosomes in response to nimotuzumab while

low-expressed TE-1 cells had not been. Therefore, autophagy induction by nimotuzumab is most likely to be mediated through pathways downstream of EGFR, such as MEK/Erk and class-I PI3K/Akt/mTOR pathways.[26,27] Cetuximab has been indicated to induce autophagy via inhibition of the class-I PI3K/Akt/mTOR pathway in the vulvar squamous carcinoma cell line A431.[28] Thus, additional testing on the activation of these EGFR downstream pathways are needed in order to further understand the mechanism whereby nimotuzumab promotes autophagy in our later work.

Conclusions

In conclusion, our results strongly suggest that nimotuzumab-combined therapy might be more beneficial for treating ESCC patients with a high level of EGFR expression, due to autophagic activation mediated by nimotuzumab to promote autophagic cell death. In addition, activation of autophagy as part of a combined therapy may be an alternative approach to kill cancer cells more efficiently.

Author contributions: HS and BP contributed equally to this work. LC designed and guided the study. HS performed all the cytology tests and part of molecular biology experiments. BP performed Western blot test, IHC, and siRNA test. JY did transmission electron microscopy test and performed the statistical analysis. HS and BP drafted the manuscript. All authors read and approved the final manuscript.

ACKNOWLEDGMENTS

This work was supported by the National Natural Science Foundation of China (Grant Nos. 81071806, 81172106 and 81301914) and the Natural Science Foundation of Jiangsu Province (Grant NO.BK.2012371).

REFERENCES

1. Jemal A. Global cancer statistics. *CA Cancer J Clin* 2011;**61**:134
2. Park BB, Im YH, Hwang IG, Lee SC, Ahn JS, Ahn MJ, Lim HY, Kang WK, Park K. Salvage chemotherapy with mitomycin C, ifosfamide, and cisplatin (MIC) for previously treated metastatic or recurrent esophageal squamous cell carcinoma. *Invest New Drugs* 2008;**26**:387–92
3. Jin J, Xu X, Wang F, Yan G, Liu J, Lu W, Li X, Tucker SJ, Zhong B, Cao Z, Wang D. Second-line combination chemotherapy with docetaxel and nedaplatin for Cisplatin-pretreated refractory metastatic/recurrent esophageal squamous cell carcinoma. *J Thorac Oncol* 2009;**4**:1017–21
4. Tepper J, Krasna MJ, Niedzwiecki D, Hollis D, Reed CE, Goldberg R, Kiel K, Willett C, Sugarbaker D, Mayer R. Phase III trial of trimodality therapy with cisplatin, fluorouracil, radiotherapy, and surgery compared with surgery alone for esophageal cancer: CALGB 9781. *J Clin Oncol* 2008;**26**:1086–92
5. Gibault L, Metges JP, Conan-Charlet V, Lozac'h P, Robaszkiewicz M, Bessaguet C, Lagarde N, Volant A. Diffuse EGFR staining is associated with reduced overall survival in locally advanced oesophageal squamous cell cancer. *Br J Cancer* 2005;**93**:107–15
6. Wilkinson NW, Black JD, Roukhadze E, Driscoll D, Smiley S, Hoshi H, Geradts J, Javle M, Brattain M. Epidermal growth factor receptor expression correlates with histologic grade in resected esophageal adenocarcinoma. *J Gastrointest Surg* 2004;**8**:448–53
7. Rosell R, Vergnenegre A, Liu B, Cobo M, Massuti B, Wei J, Molina MA, Costa C, Queralt C, Taron M. Biomarkers in lung oncology. *Pulm Pharmacol Ther* 2010;**23**:508–14
8. Chakravarti A, Winter K, Wu CL, Kaufman D, Hammond E, Parliament M, Tester W, Hagan M, Grignon D, Heney N, Pollack A, Sandler H, Shipley W. Expression of the epidermal growth factor receptor and Her-2 are predictors of favorable outcome and reduced complete response rates, respectively, in patients with muscle-invading bladder cancers treated by concurrent radiation and cisplatin-based chemotherapy: A report from the Radiation Therapy Oncology Group. *Int J Radiat Oncol Biol Phys* 2005;**62**:309–17
9. Vordermark D, Kolbl O. Lack of survival benefit after stereotactic radiosurgery boost for glioblastoma multiforme: Randomized comparison of stereotactic radiosurgery followed by conventional radiotherapy with carmustine to conventional radiotherapy with carmustine for patients with glioblastoma multiforme: Report of radiation therapy oncology group 93-05 protocol: In regard to Souhami et al. *Int J Radiat Oncol Biol Phys* 2005;**62**:296–7
10. Yang Z, Klionsky DJ. Eaten alive: A history of macroautophagy. *Nat Cell Biol* 2010;**12**:814–22
11. Levine B, Kroemer G. Autophagy in aging, disease and death: the true identity of a cell death impostor. *Cell Death Differ* 2009;**16**:1–2
12. Talavera A, Friemann R, Gomez-Puerta S, Martinez-Fleites C, Garrido G, Rabasa A, Lopez-Requena A, Pupo A, Johansen RF, Sanchez O, Krengel U, Moreno E. Nimotuzumab, an antitumor antibody that targets the epidermal growth factor receptor, blocks ligand binding while permitting the active receptor conformation. *Cancer Res* 2009;**69**:5851–9
13. Crombet T, Osorio M, Cruz T, Roca C, del Castillo R, Mon R, Iznaga-Escobar N, Figueredo R, Koropatnick J, Renginfo E, Fernandez E, Alvarez D, Torres O, Leonard I, Perez R, Lage A. Use of the humanized anti-epidermal growth factor receptor monoclonal antibody h-R3 in combination with radiotherapy in the treatment of locally advanced head and neck cancer patients. *J Clin Oncol* 2004;**22**:1646–54
14. Ramos TC, Figueredo J, Catala M, Gonzalez S, Selva JC, Cruz TM, Toledo C, Silva S, Pestano Y, Ramos M, Leonard I, Torres O, Marinello P, Perez R, Lage A. Treatment of high-grade glioma patients with the humanized anti-epidermal growth factor receptor (EGFR) antibody h-R3: Report from a phase I/II trial. *Cancer Biol Ther* 2006;**5**:375–9
15. Huang Y, Yu T, Fu X, Chen J, Liu Y, Li C, Xia Y, Zhang Z, Li L. EGFR inhibition prevents in vitro tumor growth of salivary adenoid cystic carcinoma. *BMC Cell Biol* 2013;**14**:13
16. Zhao L, Li QQ, Zhang R, Xi M, Liao YJ, Qian D, He LR, Zeng YX, Xie D, Liu MZ. The overexpression of IGFBP-3 is involved in the chemosensitivity of esophageal squamous cell carcinoma cells to nimotuzumab combined with cisplatin. *Tumour Biol* 2012;**33**:1115–23
17. Slee EA, Zhu H, Chow SC, MacFarlane M, Nicholson DW, Cohen GM. Benzyloxycarbonyl-Val-Ala-Asp (OMe) fluoromethylketone (Z-VAD.FMK) inhibits apoptosis by blocking the processing of CPP32. *Biochem J* 1996;**315**:21–4
18. Jin S, White E. Role of autophagy in cancer: management of metabolic stress. *Autophagy* 2007;**3**:28–31
19. Das AK, Chen BP, Story MD, Sato M, Minna JD, Chen DJ, Nirodi CS. Somatic mutations in the tyrosine kinase domain of epidermal growth factor receptor (EGFR) abrogate EGFR-mediated radioprotection in non-small cell lung carcinoma. *Cancer Res* 2007;**67**:5267–74
20. Fung C, Chen X, Grandis JR, Duvvuri U. EGFR tyrosine kinase inhibition induces autophagy in cancer cells. *Cancer Biol Ther* 2012;**13**:1417–24
21. Li X, Lu Y, Pan T, Fan Z. Roles of autophagy in cetuximab-mediated cancer therapy against EGFR. *Autophagy* 2010;**6**:1066–77
22. Diaz Miqueli A, Rolff J, Lemm M, Fichtner I, Perez R, Montero E. Radiosensitisation of U87MG brain tumours by anti-epidermal growth factor receptor monoclonal antibodies. *Br J Cancer* 2009;**100**:950–8
23. Akashi Y, Okamoto I, Iwasa T, Yoshida T, Suzuki M, Hatashita E, Yamada Y, Satoh T, Fukuoka M, Ono K, Nakagawa K. Enhancement of the antitumor activity of ionising radiation by nimotuzumab, a humanised monoclonal antibody to the epidermal growth factor receptor, in non-small cell lung cancer cell lines of differing epidermal growth factor receptor status. *Br J Cancer* 2008;**98**:749–55

24. Garrido G, Tikhomirov IA, Rabasa A, Yang E, Gracia E, Iznaga N, Fernandez LE, Crombet T, Kerbel RS, Perez R. Bivalent binding by intermediate affinity of nimotuzumab: A contribution to explain antibody clinical profile. *Cancer Biol Ther* 2011;**11**:373–82
25. Chu Q, Amano O, Kanda Y, Kunii S, Wang Q, Sakagami H. Tumor-specific cytotoxicity and type of cell death induced by gefitinib in oral squamous cell carcinoma cell lines. *Anticancer Res* 2009;**29**:5023–31
26. Li X, Luwor R, Lu Y, Liang K, Fan Z. Enhancement of antitumor activity of the anti-EGF receptor monoclonal antibody cetuximab/C225 by perifosine in PTEN-deficient cancer cells. *Oncogene* 2006;**25**:525–35
27. Lu Y, Li X, Liang K, Luwor R, Siddik ZH, Mills GB, Mendelsohn J, Fan Z. Epidermal growth factor receptor (EGFR) ubiquitination as a mechanism of acquired resistance escaping treatment by the anti-EGFR monoclonal antibody cetuximab. *Cancer Res* 2007;**67**:8240–7
28. Li X, Fan Z. The epidermal growth factor receptor antibody cetuximab induces autophagy in cancer cells by downregulating HIF-1alpha and Bcl-2 and activating the beclin 1/hVps34 complex. *Cancer Res* 2010;**70**:5942–52

(Received July 27, 2013, Accepted January 16, 2014)